Journal of Applied Polymer Science

Breathable Properties of *m*-Aramid Nanofibrous Membrane with High Thermal Resistance

Young Shin Park,[1] Jong Wha Lee,[1] Young Sik Nam,[2] Won Ho Park[1]

[1]Department of Advanced Organic Materials and Textile System Engineering, Chungnam National University, Daejeon 305-764, South Korea

[2]Goostech Co., Daejeon 305-764, South Korea

Correspondence to: W. H. Park (E-mail: parkwh@cnu.ac.kr)

ABSTRACT: Electrospinning of *m*-aramid in dimethyl acetamide/LiCl solution was investigated to develop thermo-resistant nanofibrous membranes for breathable waterproof materials. The *m*-aramid nanofibers were continuously generated and densely mounted to the membrane without the blockage of the spinning tip during electrospinning. In order to obtain the electrospun *m*-aramid nanofibers with different fiber diameters, the polymer concentration in the solution and the spinning distance were varied. Electrospun *m*-aramid nanofibrous membranes of various fiber diameters and thicknesses were prepared, and then compared with two commercial expanded polytetrafluoroethylene (ePTFE) membranes with respect to water vapor permeability and pore size. The *m*-aramid nanofibrous membrane showed a good water vapor permeability that satisfied the criterion of a breathable membrane, higher than those of the ePTFE porous membranes. Therefore, *m*-aramid nanofibrous membrane with thermal and mechanical resistance has great potential for breathable waterproof materials and filters. © 2014 Wiley Periodicals, Inc. J. Appl. Polym. Sci. **2015**, *132*, 41515.

KEYWORDS: electrospinning; membranes; separation techniques

Received 22 July 2014; accepted 12 September 2014

DOI: 10.1002/app.41515

INTRODUCTION

Poly(*meta*-phenylene isophthalamide), which is known by the commercial name *meta*-aramid (*m*-aramid), is a promising high performance polymer with good thermal and mechanical properties such as chemical resistance, heat and flame resistance, high tensile strength, and toughness.[1,2] *m*-Aramid fibers have been widely used in fire resistant clothing, protective clothing, fiber filters of high temperature, and insulation paper, because of higher performance/price ratio than other fibers with high thermal resistance.

Electrospinning, a new class of fiber spinning, has recently attracted much attention in material science and engineering as a potential nanotechnology for various applications, particularly for filters. A nanofibrous structure is thought to enhance filtration performance. Polymer nanofibers exhibiting high surface-to-volume and length-to-diameter ratios can be easily prepared by electrospinning. These characteristics are essential for various advanced applications, such as separation membranes, wound dressing materials, artificial blood vessels, sensors, composite reinforcements, etc.[3–7] Recently, the electrospinning technique has been employed to prepare micro- or nanoporous *p*- or *m*-aramid membranes.[8–11] Electrospinning of *p*-aramid was first carried out by Srinivan and Reneker.[8] In their studies, nanofibers with diameters ranging from 40 nm to several hundred nanometers were produced. However, morphology and mechanical properties of the deposited nanofibers were not reported, maybe because a continuous electrospinning was not feasible. In the case of *m*-aramid, it was also difficult to fabricate nanofibrous membranes via a continuous electrospinning. However, its electrospinnability was improved by adding specific salts such as LiCl and $CaCl_2$ to dimethyl acetamide (DMAc) solvent.[9,10] Based on this approach, morphological and mechanical properties of electrospun *m*-aramid nanofibers with different solvent systems were mainly studied. Wei et al. studied adsorption properties of electrospun *m*-aramid nanofibers using methylene blue (MB) as a model compound.[11] They found that aramid nanofibers had a faster adsorption rate for MB from its aqueous solution, compared with activated carbon. On the contrary, the specific applications for *m*-aramid nanofibrous membrane are challenging because it has high thermal stability due to a rigid molecular structure.

In this study, we investigate the *m*-aramid nanofibrous membrane with thermal resistance for breathable waterproof materials. Uniform fiber structure and diameter are obtained. Consequently, the pore structure of the nanofibrous membrane is controlled to obtain the desired breathable properties. For this, *m*-aramid is electropun under controlled experimental

conditions. The changes in fiber diameter and morphology are investigated for different spinning conditions (polymer concentration, applied voltage, and spinning distance). Electrospun *m*-aramid nanofibrous membranes with various fiber diameters and membrane thicknesses are prepared, and then compared to expanded polytetrafluoroethylene (ePTFE) membranes in terms of water vapor permeability and pore parameters.

EXPERIMENTAL

Materials

m-Aramid was provided as a 18 wt % solution by Huvis Co. (Korea), which was diluted to 15 wt % using DMAc for electrospinning. DMAc was purchased from Aldrich Co. (USA) and used as received. The extended polytetrafluoroethylene (ePTFE-O) film and the ePTFE film chemically treated with hydrophilic polyurethane (ePTFE-C) were kindly supplied by GE Co. (USA).

Electrospinning

The electrospinning setup used in this study consisted of a syringe and needle (18–24 G, ID = 0.838–0.318 mm), a ground electrode ($d = 21.5$ cm, stainless steel sheet on a drum whose rotation speed can be varied), and a high voltage supply (Chungpa EMT, CPS-40K03). The needle was connected to the high voltage supply, which can generate positive DC voltages up to 40 kV. For the electrospinning, *m*-aramid solutions in DMAc were prepared in concentrations ranging 9–18 wt % and delivered by a syringe pump (KD Scientific, Model 100) at a mass flow rate of 0.5–1.5 mL/h. The distance between the needle tip and the ground electrode was in a range of 10–20 cm, and the positive voltage applied to polymer solutions were in a range of 15–25 kV. All experiments were carried out at constant temperature and humidity (25 ± 1°C, 40 ± 3%).

Measurement and Characterization

The morphology of the electrospun *m*-aramid nanofibers was observed with a scanning electron microscope (SEM) (Hidachi S-2350). Samples for SEM were dried under vacuum, mounted on metal stubs, and sputter-coated with gold for 30–60 s. The average diameter and its distribution of the electrospun fibers were obtained by analyzing the SEM images with a custom code image analysis program (Scope Eye II). The thickness of the *m*-aramid nanofibrous membrane was measured on a compression-type thickness tester (ID-S112, Mitutoyo Co, Japan) because the nanofibrous membrane had a very rough surface, and presented as an average value with standard deviation after measurement across 30 points for each sample. The pore size and its distribution of the *m*-aramid nanofibrous membrane were measured by the Automated Capillary Flow Porometer (CFP-1200-AEL, Porous Materials Inc.) according to ASTM F316. Water vapor permeability was measured in a constant temperature and humidity chamber (TH-M-025, Jeio Tech, Korea) according to KS K 0594 (calcium chloride method). Permeability (g/m^2 day) was obtained at constant temperature and humidity (40 ± 2°C, 90 ± 5%) using the following equation.

$$\text{Permeability } (P) = (a_2 - a_1/S) \times 24$$

where a_1: weight of sample after 1 h, a_2: weight of sample after 2 h, and S: sample area.

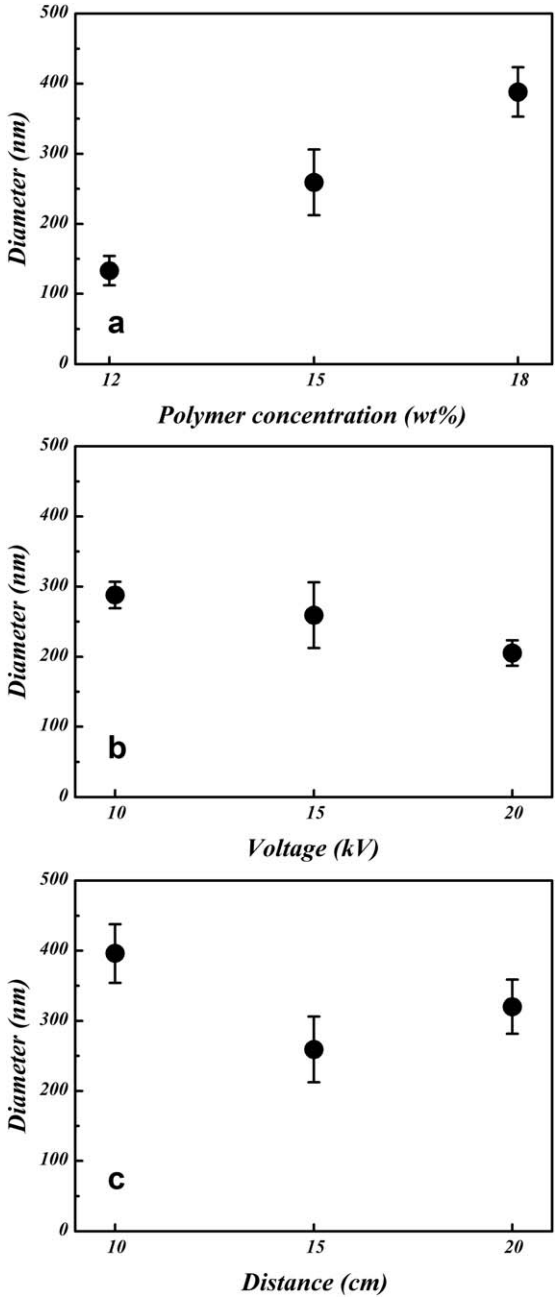

Figure 1. Average fiber diameters of *m*-aramid nanofibers for different process conditions.

Thermal properties were measured by a thermogravimetric analyzer (Pyris 1, PerkinElmer). The sample was heated to 800°C at a heating rate of 10 °C/min under nitrogen atmosphere. Shrinkage (%) in hot air was obtained by comparing the sample area (original: 35 mm^2) before and after heat treatment at temperatures of 200, 250, 300, and 350°C for 30 min.[12,13]

RESULTS AND DISCUSSION

Fiber Diameter of *m*-Aramid Nanofibers with Different Spinning Parameters

In electrospinning, the solution viscosity plays an important role in determining the range of concentrations from which

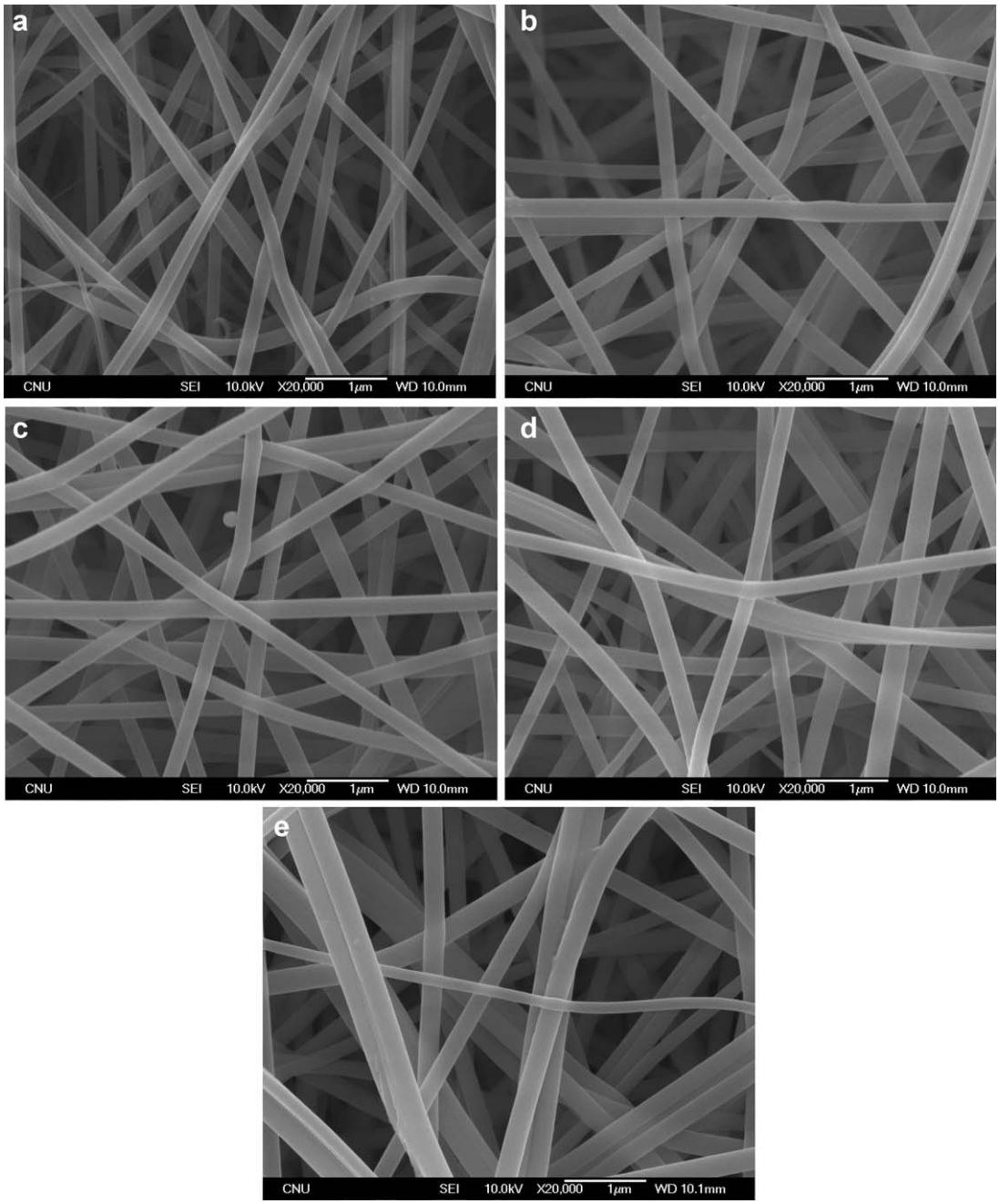

Figure 2. SEM micrographs of *m*-aramid nanofibers electrospun at different conditions (20,000×). Electrospinning conditions; polymer concentration = 15 wt %, applied voltage = 15–25 kV, flow rate = 0.1–1.0 mL/min, spinning distance = 15 cm.

continuous fibers can be obtained. A continuous fiber is formed from the extensive chain entanglements in polymer solution. Figure 1 shows the changes in the diameter of the *m*-aramid nanofibers according to polymer concentration, applied voltage, and spinning distance. As the concentration of the *m*-aramid solution increased, the fiber diameter increased gradually [Figure 1(a)]. As the jet leaves the needle tip during electrospinning, the polymer solution is stretched until it reaches the collector. If the amount of entanglement of the polymer chains in the solution is sufficient to form the continuous fibers, the viscosity of the solution (polymer concentration) affects the extent of elongation of the ejected jets. Subsequently, the diameter of *m*-aramid nanofibers was increased with the increase in the *m*-aramid concentration because the greater amount of entanglement in solution inhibited the elongation of jets. In contrast, as the applied voltage increased, the fiber diameter slightly decreased [Figure 1(b)]. When the applied voltage is higher, the greater amount of charges caused the jet to stretch faster, resulting in fiber formation with a smaller diameter. With respect to spinning distance, the fiber diameter of the *m*-aramid nanofibers showed a minimum value at distance of 15 cm, but its deviation was not significant. Therefore, no significant effect of the

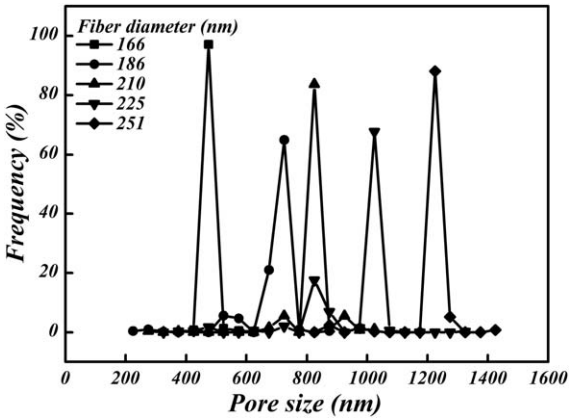

Figure 3. Pore size distributions of *m*-aramid nanofibrous membranes with different fiber diameters.

distance between the tip and collector on the fiber diameter was observed. Figure 2 shows SEM micrographs of the *m*-aramid nanofibers electrospun at different conditions. The average diameters of the electrospun *m*-aramid obtained at different spinning conditions were in the narrow range of 166–251 nm. The electrospun *m*-aramid fibers were uniform and mounted straight.

Pore Size of *m*-Aramid Nanofibrous Membrane for Different Fiber Diameters and Membrane Thicknesses

Pore structures of various sizes and shapes were generated in the electrospun nanofibrous membrane. Pores provide channels for water vapor transport, and thus their size and distribution have an important effect on water vapor permeability.[14] Figure 3 shows the pore size distributions of *m*-aramid nanofibrous membranes of different fiber diameters (average membrane thickness = 9.1 μm). The nanofibrous membranes have macropores ranging from 480 to 1250 nm, and their pore sizes increase with increasing fiber diameter. Also, pore size distribution is very narrow, regardless of the fiber diameter. Figure 4 shows the pore size distributions of *m*-aramid nanofibrous membranes (average fiber diameter = 166 nm) with different membrane thicknesses. As the membrane thickness increases, the pore size gradually decreases. No significant decrease in

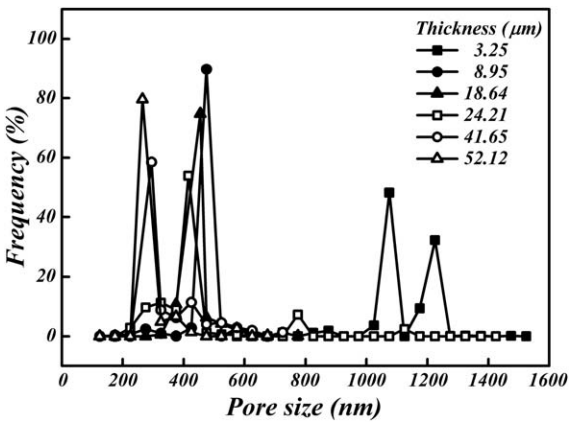

Figure 4. Pore size distributions of *m*-aramid nanofibrous membranes with different thicknesses.

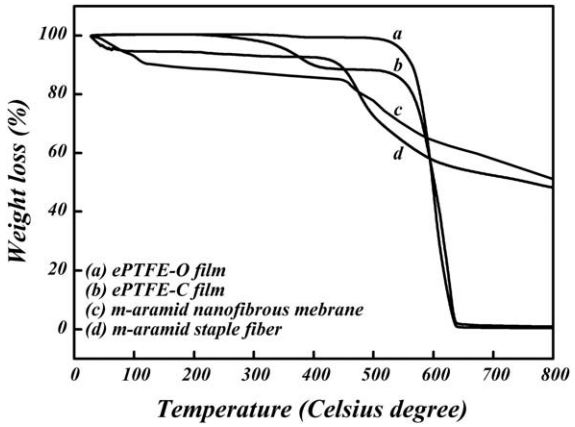

Figure 5. TGA thermograms of ePTFE films, *m*-aramid staple fiber, and *m*-aramid nanofibrous membranes. Electrospinning conditions of *m*-aramid; polymer concentration = 15 wt %, applied voltage = 15 kV, spinning distance = 15 cm.

pore size is observed above the thickness of 8.95 μm. Therefore, the pore size of a nanofibrous membrane is affected by both the fiber diameter and the membrane thickness. Noticeably, this narrow pore size distribution might be desirable for improved water vapor barrier properties.

Thermal Stability of *m*-Aramid Nanofibrous Membrane

The thermal stability of high thermo-resistant polymers was evaluated by the glass transition temperature (T_g), crystalline melting temperature (T_m), and thermal decomposition temperature (T_d).[15] Figure 5 shows the thermogravimetric analysis (TGA) thermograms of the ePTFE-O, ePTFE-C, *m*-aramid membrane, and *m*-aramid staple fiber (provided by Huvis Co.). The weight decrease at around 100°C was due to the evaporation of residual moisture and/or solvent, and the weight losses at 430–450°C and at 550°C were associated with the chain scission of the *m*-aramid polymer and the backbone chain scission of the PTFE polymer, respectively. In the case of ePTFE-C, the weight loss at around 250°C might be caused by the degradation of the polyurethane chain, which was used for after-treatment of PTFE. Particularly, the degradation behavior of the electrospun *m*-aramid membrane was similar to that of the staple fiber, and the residual weight of *m*-aramid membrane at 800°C was approximately 50% (the actual residual weight at 800°C was −64% when the initial weight loss of solvent and

Table I. Changes in Shrinkage (%) of ePTFE-O, ePTFE-C, and *m*-Aramid Nanofibrous Membranes After Heat Treatment

	Thermal shrinkage (%)		
Temperature/ Time	*m*-Aramid nanofibrous membrane	ePTFE-O film	ePTFE-C film
200°C/0.5 h	7.51	33.4	38.9
250°C/0.5 h	10.8	42.8	43.4
300°C/0.5 h	21.8	55.7	48.6
350°C/0.5 h	50.4	79.4	77.1

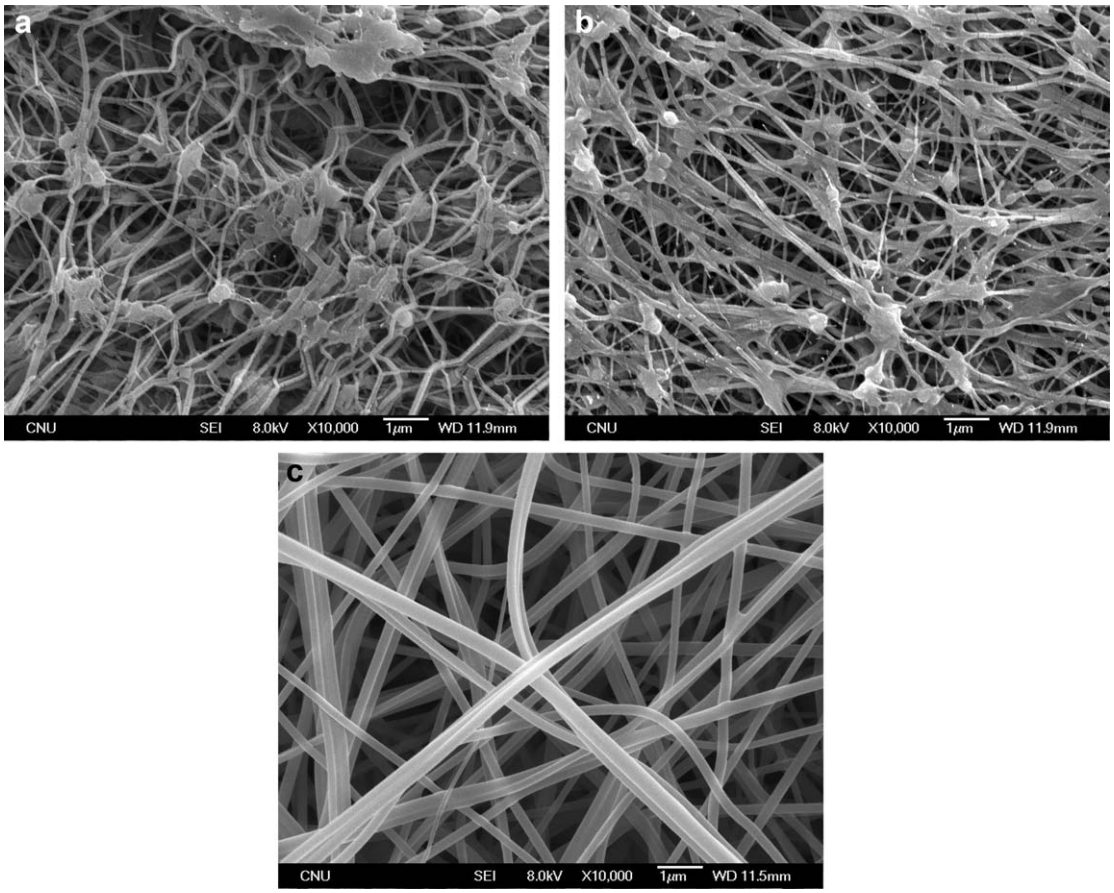

Figure 6. SEM images of ePTFE-O, ePTFE-C, and *m*-aramid nanofibrous membranes (10,000×). Electrospinning conditions of *m*-aramid; polymer concentration = 15 wt %, applied voltage = 15 kV, spinning distance = 15 cm.

moisture was excluded), whereas the two ePTFE samples were completely degraded at around 600°C.

Table I shows the changes in shrinkage (%) of ePTFE-O, ePTFE-C, and *m*-aramid nanofibrous membranes with heat treatment temperature. Heat treatment was performed in the range of 200–350°C for 30 min. The shrinkage (%) was calculated as the area of heat-treated sample divided by the original sample area (35 mm^2). As the heat treatment temperature increased from 200 to 350°C, the shrinkage (%) of *m*-aramid membrane increased from 7.5% to 50.4%, while those of the two PTFE samples increased from about 35% to about 78%. After the heat treatment at 300°C, the color of the ePTFE-C membrane became brownish. Therefore, the *m*-aramid nanofibrous membrane showed higher thermal stability than the two ePTFE membranes.

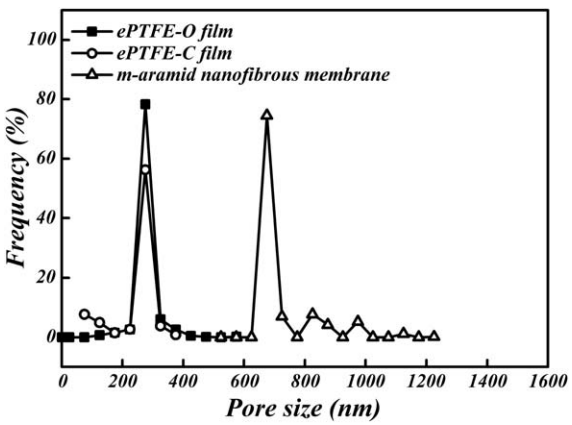

Figure 7. Pore size distributions of ePTFE-O, ePTFE-C, and *m*-aramid nanofibrous membranes.

Water Vapor Permeability of *m*-Aramid Nanofibrous Membrane

Figure 6 shows SEM images of the ePTFE-O, ePTFE-C, and *m*-aramid membranes. The ePTFE membranes had a beaded fibril-like structure, and particularly ePTFE-C had slightly smaller pores than ePTFE-O. The pore sizes and their distributions of ePTFE-O, ePTFE-C, and *m*-aramid nanofibrous membranes with similar membrane thicknesses and gram per square meter (GSM) values are compared in Figure 7. The pore sizes of ePTFE-O and ePTFE-C were 287 nm and 256 nm, respectively, indicating that the pore size of ePTFE was slightly decreased by hydrophilic polyurethane treatment. On the contrary, the pore size of the *m*-aramid nanofibrous membrane was 647 nm.

Water vapor permeability is closely related to capability releasing the sweat generated from human body, and thus is an essential parameter affecting amenity. Generally, water the minimum value of vapor permeability of breathable waterproof

Table II. Water Vapor Permeability Values of ePTFE-O, ePTFE-C, and *m*-Aramid Nanofibrous Membranes

Type	Diameter (nm)	Thickness (μm)	GSM (g/m^2)	Permeability (g/m^2 day)	
				Specification	Experiment
ePTFE-O film	-	21–23	19	8322	8080
ePTFE-C film	-	25–30	21	7564	7711
m-Aramid nanofibrous membrane	248 ± 13	23.91 ± 0.33	21.25 ± 0.17	-	7650
None	-	-	-	-	18,808

None: test without sample.

clothing should be 4000 g/m^2 day.[16] To evaluate the water vapor permeability of the *m*-aramid membrane, the commercial ePTFE membranes (ePTFE-O, ePTFE-C) were used as references. The structural parameters of the sample membranes are summarized in Table II. The *m*-aramid and ePTFE samples of similar thicknesses and membrane densities were used. Figure 8 shows the water vapor permeability values of the ePTFE-O, ePTFE-C, and *m*-aramid membranes. The ePTFE-O membrane showed a slightly higher permeability (8080 g/m^2 day) value than the ePTFE-C membrane (7711 g/m^2 day). This may be due to the difference in pore size between ePTFE-O and ePTFE-C (Figure 7). Also, the *m*-aramid nanofibrous membrane showed a similar water vapor permeability value (7650 g/m^2 day) to those of the two ePTFE membranes, although the pore size of the *m*-aramid nanofibrous membrane was two times larger than those of the ePTFE samples. This might be due to the complex pore structure of the *m*-aramid nanofibrous membrane.

CONCLUSIONS

The heat-resistant *m*-aramid nanofibrous membrane for breathable materials was obtained by electrospinning of *m*-aramid/DMAc, and compared to ePTFE films with similar GSM and thickness in terms of water vapor permeability, pore parameters, and thermal properties. The pore size of the *m*-aramid nanofibrous membrane increased with increasing fiber diameter and decreasing membrane thickness. The *m*-aramid nanofibrous membrane had excellent thermal stability, compared with the commercial ePTFE membranes. The *m*-aramid nanofibrous membrane showed similar water permeability to the two ePTFE films. In conclusion, the *m*-aramid nanofibrous membrane of high thermal resistance has great potential for permeable water proof materials and filters.

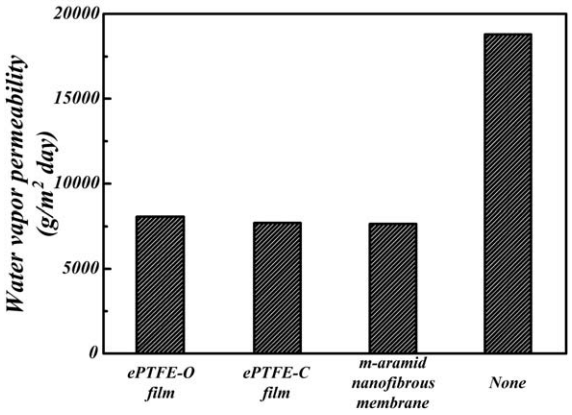

Figure 8. Water vapor permeability values of ePTFE-O, ePTFE-C, and *m*-aramid nanofibrous membranes (None: test without sample).

ACKNOWLEDGMENTS

This work was supported by the Industrial Strategic Technology Development Program (10040033) funded by the Ministry of Knowledge Economy (MKE), Korea.

REFERENCES

1. Allegra, G. *Polym. Eng. Sci.* **1975**, *15*, 207.
2. Villar-Rodil, S.; Paredes, J. I.; Martines-Alonso, A.; Tascon, J. M. D. *J. Therm. Anal. Calorim.* **2002**, *70*, 37.
3. Ramakrishna, S.; Fujihara, K.; Teo, W. E.; Yong, T.; Ma, Z.; Ramaseshan, R. *Mater. Today* **2006**, *9*, 40.
4. Han, S. O.; Youk, J. H.; Min, K. D.; Kang, Y. O.; Park, W. H. *Mater. Lett.* **2008**, *62*, 759.
5. Bai, H.; Zhao, L.; Lu, C.; Li, C.; Shi, G. *Polymer* **2009**, *50*, 3292.
6. Frenot, A.; Chronakis, I. S. *Curr. Opin. Colloid Interface Sci.* **2003**, *8*, 64.
7. Norman, J. J.; Desai, T. *Ann. Biomed. Eng.* **2006**, *34*, 89.
8. Srinivasan, G.; Reneker, D. H. *Polym. Int.* **1995**, *36*, 195.
9. Yao, L.; Lee, C.; Kim, J. *Fiber Polym.* **2010**, *11*, 1032.
10. Oh, H. J.; Pant, H. R.; Kang, Y. S.; Jeon, K. S.; Pant, B.; Kim, C. S.; Kim, H. Y. *Polym. Int.* **2012**, *61*, 1675.
11. Wei, Z.; Zhang, Q.; Wang, L.; Peng, M.; Wang, X.; Long, S.; Yang, J. *J. Polym. Sci. Polym. Phys.* **2012**, *50*, 1414.
12. Jeong, H. S.; Kim, J. H.; Lee, S. Y. *J. Mater. Chem.* **2010**, *20*, 9180.
13. Fu, D.; Luan, B.; Argue, S.; Bureau, M. N.; Davison, I. J. *J. Power Source* **2012**, *206*, 325.
14. Gibson, P.; Schreuder-Gibson, H.; Riven, D. *Colloid Surf. A* **2001**, *187–188*, 469.
15. Chae, H. G.; Kumar, S. *J. Appl. Polym. Sci.* **2006**, *100*, 791.
16. Koo, K.; Park, Y. M.; Choe, J. D.; Kim, E. A. *Polym. Eng. Sci.* **2009**, *49*, 1151.